Catalysis Today 146 (2009) 87–95

Contents lists available at ScienceDirect

Catalysis Today

journal homepage: www.elsevier.com/locate/cattod

Steam reforming of ethanol over nickel molybdenum carbides for hydrogen production

Yukihiro Miyamoto, Masato Akiyama, Masatoshi Nagai *

Graduate School of Bio-Applications and Systems Engineering, Tokyo University of Agriculture and Technology, 2-24 Naka-cho, Koganei, Tokyo 184-8588, Japan

ARTICLE INFO

Article history:
Available online 28 February 2009

Keywords:
Hydrogen production
Ethanol
NiMo carbide
CO adsorption
XRD
X-ray photoelectron spectroscopy
Temperature-programmed surface reaction

ABSTRACT

The steam reforming of ethanol over carburized NiMo catalysts was studied to determine the effects of the Ni content, carburization temperature in 20% CH_4/H_2, GHSV, potassium addition and a comparison of the reduced catalyst. The catalysts were characterized by CO adsorption, XRD, X-ray electron spectroscopy (XPS) and temperature-programmed surface reaction after ethanol adsorption. The 798 K-carburized NiMo catalyst gradually increased below 500 min and it exhibited a higher activity than the reduced NiMo catalyst. The addition of potassium promoted more hydrogen selectivity than the non-potassium-added catalysts. The 798 K-carburized catalyst exhibited the high intensity peaks of MoO_2 and small peaks of β-Mo_2C and Ni metal (or NiMo) were present, while the 823 K-carburized catalyst showed broad and small peaks. The 873 and 848 K-carburized catalysts contained a strong intensity of β-Mo_2C and clear Ni metal (or NiMo). The XPS measurements revealed that the hydrogen production was proportional to Ni^0 of the carburized NiMo catalyst. The addition of potassium significantly increases the Ni^0 ratio, which was stabilized instead of increasing the Mo oxidation during the reaction.

1. Introduction

The steam reforming of ethanol produces hydrogen and CO_2. Many researchers are investigating biomass, especially bioethanol, as a material for hydrogen production [1]. There are many studies of hydrogen production over Ni [2–10], Co [11] and Rh [12,13] on supports, such as Al_2O_3, SiO_2, CeO_2–ZrO_2, Y_2O_3, MgO and carbon nanotubes. Nickel-containing catalysts are reported to have a high activity for ethanol steam reforming and cleavage of the C–C bond. For transition metal carbides, their application extends over a wide range. Molybdenum carbide has a high surface area and also exhibits high activities for the hydrogenation of CO [14], reforming of methane and the water gas shift reaction [15–19], so it has the catalytic potential for hydrogen production. However, there are few studies of ethanol steam reforming over molybdenum carbides with potassium addition. Barthos et al. [20] reported that Mo_2C catalysts deposited on carbon (Norit Co.) and carbon nanotubes exhibited a high activity for the steam reforming of ethanol [8]. The alkali metal provides electrons to the molybdenum carbides [6,8,21], so as a result, the Mo metal atom is expected to activate, or it easily reacts with a non-metallic atom. In this study, the carburized NiMo catalysts with and without potassium were prepared and their performance examined for the steam reforming of ethanol at 673 K. The effects of the nickel content, carburization temperature, potassium addition and comparison of the catalyst reduced in hydrogen during the steam reforming of ethanol over the carburized NiMo catalysts were studied. The surface properties of the carburized catalysts were characterized by CO adsorption, XRD, X-ray electron spectroscopy (XPS), temperature-programmed surface reaction (TPSR) after ethanol adsorption. The interaction between nickel and molybdenum during the reforming of ethanol and potassium addition was investigated, and the active species for the ethanol steam reforming was discussed.

2. Experimental

The aqueous precursors for NiMo oxides with the ratio of Ni/(Ni + Mo) were prepared in mixed aqueous solutions of $(NH_4)_6Mo_7O_{24}{\cdot}4H_2O$ as the Mo source and $Ni(NO_3)_2{\cdot}6H_2O$ as the Ni source. K_2CO_3 was used for the potassium additive effect. The precursors were dried at 293 K and calcined at 773 K for 5 h in air. The oxidized precursor (0.2 g) was loaded in a reactor, oxidized at 773 K in a stream of air for 0.5 h, treated from 723 K to a final temperature of 798, 823, 843 or 873 K in a stream of 20% CH_4/H_2 at the rate of 1 K/min, maintained at this temperature for 2 h and then cooled to room temperature in a stream of 20% CH_4/H_2 for carburization. The oxidized precursor was treated at 723 K in a stream of 100% H_2 for reduction of the catalyst as compared to the carburization. The activity measurement (catalyst gram:

* Corresponding author. Tel.: +81 42 388 7060; fax: +81 42 388 7060.
E-mail address: mnagai@cc.tuat.ac.jp (M. Nagai).

0920-5861/$ – see front matter © 2009 Elsevier B.V. All rights reserved.
doi:10.1016/j.cattod.2008.12.033

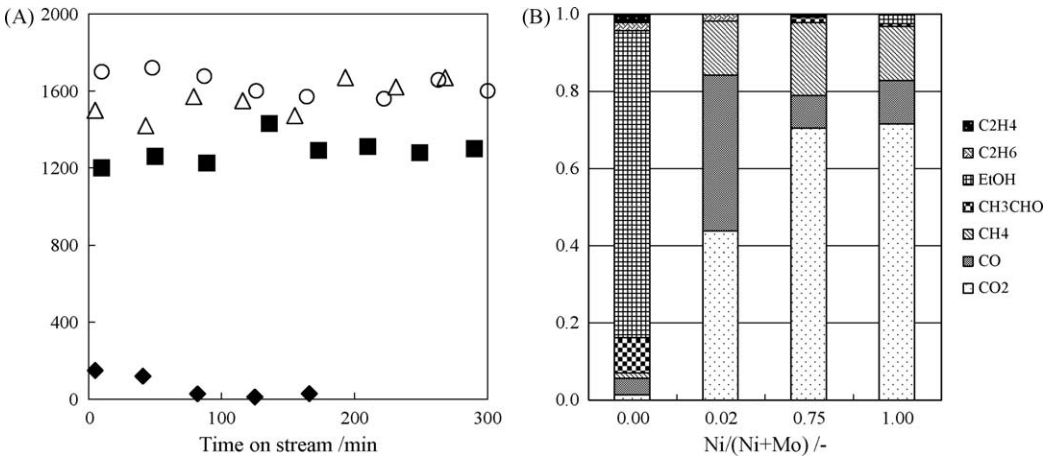

Fig. 1. (A) Formation rate of hydrogen during steam reforming of ethanol over the 823 K-carburized (◆) Mo_{100}, (■) Ni_2Mo_{98}, (△) $Ni_{25}Mo_{75}$ and (○) Ni_{100} catalysts and (B) product distribution over the 823 K-carburized catalysts with various Ni/(Ni + Mo) ratios.

0.2 g) was carried out at 673–773 K with a 1:13 mixture of ethanol and water at the flow rate of 0.02 ml/min and N_2 carrier gas at 15 ml/min. The contact time (10^{-5}–3.3×10^{-4} h) was varied with the GHSV of 3000–97,000 h^{-1}. The products were analyzed using TCD and FID-GC with a methanizer for the reaction products during the reaction. In order to determine how the carburized NiMo with and without potassium and reduced NiMo catalysts interacted with ethanol, TPSR was carried out *in situ* by heating from room temperature to 1000 K at the rate of 10 K/min in a 15 ml/min stream of Ar after ethanol (170 μmol/g-cat) was flowed over the catalysts. The H_2O (m/z = 18) was monitored using a quadruple mass spectrometer (Quadstar 422, Balzer Co.). An XRD analysis was conducted using an RINT2000 (Rigaku. Co) with Cu Kα radiation. The peaks were identified on the basis of the JCPDS card references. The XPS was performed using a Shimadzu ESCA 3200 photoelectron spectrometer with Mg Kα (1253.6 eV, 8 kV, 30 mA) at a pressure of 5×10^{-6} Pa. Argon etching was done for 1.5 min before the XPS measurement. The binding energies occurred at 227.5–228.2 eV and 230.7–231.05 eV for Mo $3d_{5/2}$ and Mo $3d_{3/2}$, respectively. Ni^0, Ni^{2+}, Ni^{3+} and Ni^{2+} satellite were measured at the binding energies occurred at 853.0 ± 0.2, 854.6, 856.0 and 861.0 ± 0.4 eV, respectively.

3. Results and discussion

3.1. Activity for ethanol steam reforming

The formation rate of hydrogen in steam reforming of ethanol over the 823 K-carburized Ni_2Mo_{98}, $N_{25}Mo_{75}$, Ni_{100} and 873 K-carburized Mo_{100} catalysts at the reaction temperature of 773 K is shown in Fig. 1. The 873 K-carburized Mo_{100} was significantly less active during the ethanol reforming. The addition of 2 mol% nickel to the Mo carbide (Ni_2Mo_{98}) extremely promoted the 6 times higher production of hydrogen versus the 873 K-carburized Mo_{100} which was more active than the 823 K-carburized Mo_{100} [18,22]. The 823 K-carburized $Ni_{25}M_{75}$ and Ni_{100} exhibited higher formation rates of hydrogen. The nickel played an important role in the steam reforming ethanol. The latter was very active in the initial stage, but equal to the former activity at 300 min. The extreme deposition of carbon after the reaction was observed for the Ni_{100} catalyst being much higher than the $Ni_{25}Mo_{75}$ and Ni_2Mo_{98} catalysts (visual measurement). It was reported that carbon had significantly accumulated on the Ni catalyst in spite of the high activity [7,23,24]. As a result, the Mo-containing nickel catalysts had less carbon accumulation probably due to the prevention of carbon accumulation by the molybdenum addition. The formation

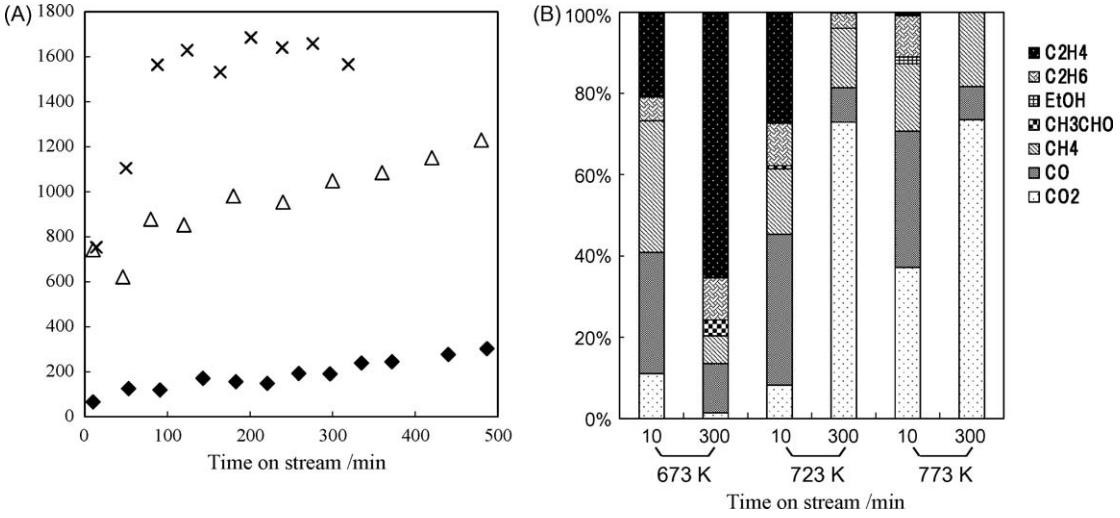

Fig. 2. (A) Formation rate of hydrogen and (B) product distribution during steam reforming of ethanol over the 823 K-carburized $Ni_{25}Mo_{75}$ at the reaction temperatures of (◆) 673, (△) 723 and (×) 773 K.

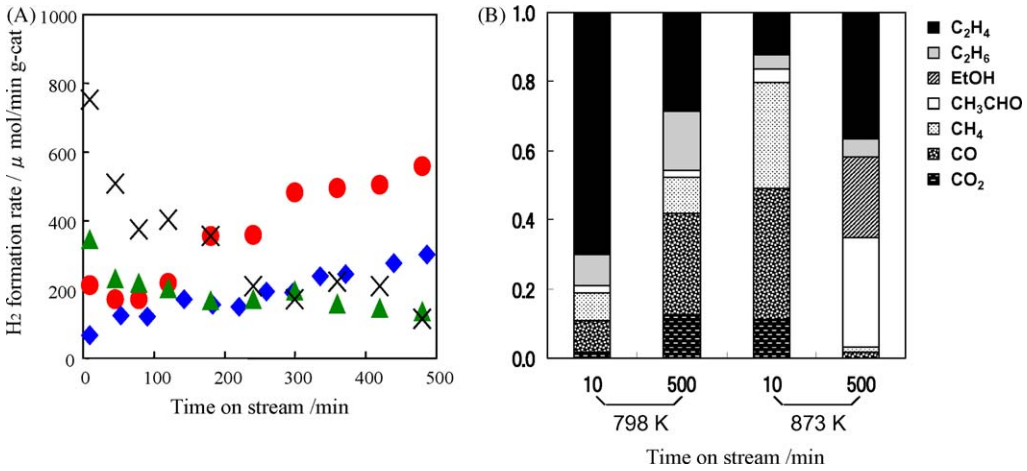

Fig. 3. (A) Formation rate of hydrogen during steam reforming of ethanol over the $Ni_{25}Mo_{75}$ catalysts carburized at (●) 798, (◆) 823, (▲) 848 and (×) 873 K and (B) product distributions over the $Ni_{25}Mo_{75}$ carburized at the 798 and 873 K.

rate of hydrogen during ethanol steam reforming over the 823 K-carburized $Ni_{25}Mo_{75}$ catalyst at the reaction temperatures of 673, 723 and 773 K is shown in Fig. 2. Ethanol was completely converted even at 673 K, but hydrogen was less formed. Ethylene by breaking of the C–O bond of ethanol was formed in high amounts along with acetaldehyde and ethanol. At the reaction temperature of 773 K, the hydrogen formation rate was the highest and CO_2 was significantly formed with methane and CO due to the C–C bond scission of acetaldehyde through the dehydrogenation of ethanol. Although the reforming catalyst should have the performance of the C–C bond rupture for a high hydrogen production, the reaction temperature of 773 K was not selected with little difference in the performance of the catalysts, but in this study, 673 K was selected for the development of the catalysts with a high hydrogen production and less ethylene formation.

The activity measurement was carried out for the $Ni_{25}Mo_{75}$ catalysts at the different carburization temperature of 673 K. The changes in the hydrogen formation rates and the product distributions at 10 and 500 min are shown in Fig. 3. As seen as a change in the hydrogen formation rate, the best performance based on the hydrogen formation rate was seen on the $Ni_{25}Mo_{75}$ catalysts carburized at 798 K (Fig. 3A). The 798 K-carburized catalyst exhibited the highest formation rate with a 27% hydrogen selectivity at 500 min. The hydrogen formation on the catalyst carburized at a lower temperature increased more with the reaction time. For the 798 K-carburized $Ni_{25}Mo_{75}$, ethylene was clearly observed during the initial step, and decreased with the reaction time along with the concomitant increase in the C1 products, especially CO. The 873 K-carburized catalyst exhibited an extremely high hydrogen formation rate with a high selectivity of CH_4 and CO during the initial stage and then decreased by 500 min. This result shows the activity for the decomposition of acetaldehyde to CH_4 and CO during the initial stage, but this activity (C–C bond scission) quickly decreased with the increasing C–O bond cleavage. Furthermore, no unconverted ethanol was observed for the 798 and 823 K-carburized catalysts until 500 min, but was significantly observed for the 873 K-carburized catalyst. As a result, the 798 K-carburized catalyst exhibited a higher ethylene selectivity and lower acetaldehyde selectivity than the catalyst carburized at 873 K. The 798 K-carburized catalyst undergoes C–O bond cleavage rather than the catalysts carburized at the higher temperatures. For the 873 K-carburized catalyst, the C–C bond of the acetaldehyde was broken only during the initial stage, but was suppressed with the increased activity for the C–O bond cleavage. As a result, the C–O bond cleavage was related to the active species of the 798 K-carburized catalyst, such as the Mo oxycarbide or oxide, and the C–C bond cleavage was related to the active species of the 873 K-carburized catalyst, such as the NiMo carbides and Ni metal (or NiMo). The change in the contact time from 10^{-5} to 3.3×10^{-4} h for the 823 K-carburized $Ni_{25}Mo_{75}$ catalyst occurred during the ethanol steam reforming. The carburized catalyst exhibited a selectivity for hydrogen production with CO, CH_4 and CO_2 at a low contact time and for those of acetaldehyde and ethylene at a high contact time (Fig. 4). These results showed that the C2 compounds were the intermediate of which the desired catalyst will promote breaking of the C–C bond. The C1 compounds were formed from the decomposition of the acetaldehyde and the C2 compounds.

3.2. Promotion of potassium addition

The activities of the $Ni_{24}Mo_{74}K_2$ catalysts carburized at 798–874 K and the product distributions of the $Ni_{24}Mo_{74}K_2$ catalysts carburized at 798 and 873 K are shown in Fig. 5. The 873 K-carburized catalyst significantly promoted the acetaldehyde selectivity, but reduced the methane formation and the ethylene selectivity by the potassium addition. The potassium-added 873 K-carburized catalyst did not exhibit a high hydrogen formation with a stable activity during the initial stage, although the catalyst without potassium showed a high hydrogen formation rate. Ethylene was selectively increased during the reaction for the

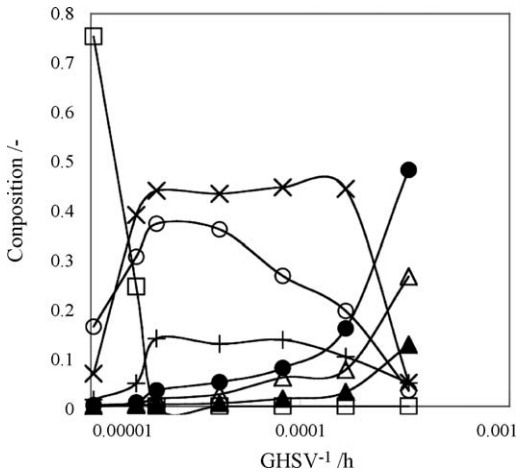

Fig. 4. Change in contact time from 10^{-5} to 3.3×10^{-4} h for the 823 K-carburized $Ni_{25}Mo_{75}$ catalyst during ethanol steam reforming at 673 K. (▲) CO_2, (●) CO, (△) CH_4, (○) CH_3CHO, (×) ethylene, (+) ethane and (□) ethanol.

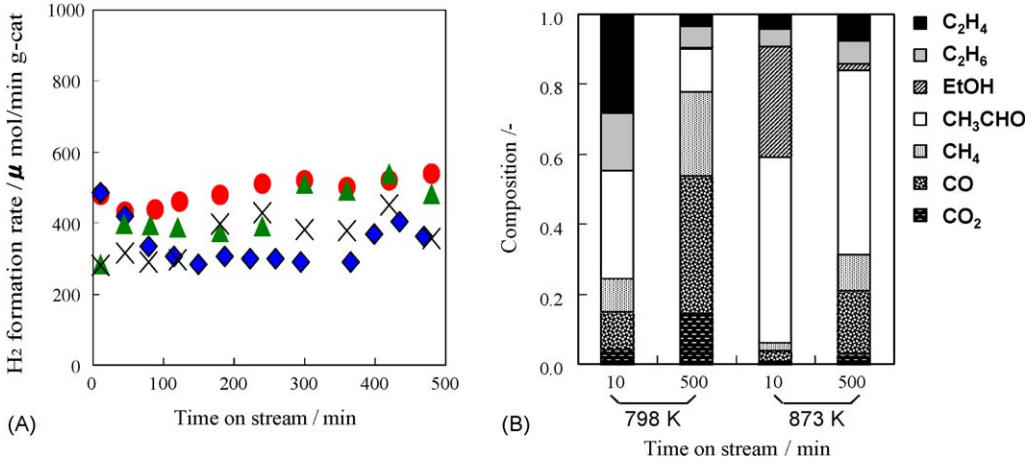

Fig. 5. (A) Formation rate of hydrogen during steam reforming of ethanol over the $Ni_{24}Mo_{74}K_2$ catalysts carburized at (●) 798, (◆) 823, (▲) 848 and (×) 873 K and (B) product distributions over the $Ni_{25}Mo_{75}$ carburized at 798 and 873 K.

873 K-carburized catalyst with and without potassium, mainly due to the oxidation of the carbides to oxides. On the other hand, the 798 K-carburized catalyst exhibited half the ethylene selectivity compared to the catalyst without potassium, but increased the CH_4 and CO selectivity after a 100-min reaction time. This result showed that the potassium addition for the 798 K-carburized catalyst decreased the C–O bond cleavage and increased the C–C bond cleavage during the reaction. As ethylene is reported to formed by acid solids [7], such as Ni and Mo oxides, the addition of potassium neutralized the acid sites [25] to promote the selectivity of the dehydrogenation of ethanol to acetaldehyde (that is, the promotion of the O–H bond scission) and to suppress the ethylene selectivity (that is, C–O bond scission). In addition, the potassium addition promoted the dissociation of water into OH and H and the subsequent dissociation of 2H and O [26]. Thus, the addition of potassium to the catalyst was effective for the O–H bond scission with a lower C–O bond scission and long and stable steam reforming reaction.

Based on these results, the steam reforming of ethanol on the catalysts carburized at 798–873 K with and without potassium occurred as a complex scheme as shown in Fig. 6. The steam reforming of ethanol proceeds with the dehydrogenation to acetaldehyde (O–H bond was broken for the 798 K-carburized catalyst without potassium in the initial stage; 798 and 873 K-carburized catalysts with potassium in the initial stage; 873 K-carburized catalyst without potassium in the final stage) or the dehydration to ethylene (C–O bond scission; extremely high for 798 K-carburized catalysts without potassium during the reaction; 873 K-carburized catalysts with and without potassium in the final stage). The C–C bond of acetaldehyde was broken and CH_4 and CO formed (C–C bond scission; 873 K-carburized catalyst without potassium in the initial stage; 798 K-carburized catalyst with potassium). Ethylene was decomposed in the steam, dehydrogenated to carbonaceous carbons ($C_2H_4 \rightarrow 2C_{surface} + 2H_2$), or hydrogenated to ethane for the hydrogen consumption. The formation of CH_4 and ethane as byproducts decreased the hydrogen selectivity. CO was a poison for the PEFC electrode catalyst, and should be reduced. For the C1 products, the water gas CO shift reaction ($CO + H_2O \rightarrow CO_2 + H_2$; 873 K without potassium in the final stage and with potassium in the initial stage) and steam reaction of methane ($CH_4 + H_2O \rightarrow CO + 3H_2$; 873 K without potassium in the final stage and with potassium in the initial stage) occurred. Thus, the 873 K-carburized catalyst is active during the water shift reaction and steam reforming.

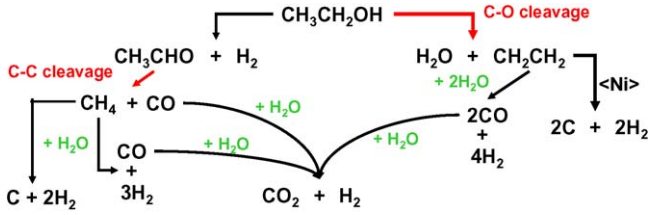

Fig. 6. Scheme of steam reforming of ethanol on carburized NiMo catalysts.

The BET surface area and CO adsorption of the catalysts are shown in Table 1. The potassium-added catalysts possessed lower surface areas than the catalysts without potassium or after the reaction, except for the 843 K-catalyst before the reaction. Zhu et al. [27] reported a decrease in the surface area of Mo_2C/Al_2O_3 by the addition of alkali metals. Furthermore, the addition of K, Na and Li to the Ni/MgO catalyst decreased the surface area and Ni dispersion and increased the particle size [4]. The CO adsorption and TOF of the catalysts for the hydrogen formation are shown in Table 1. The CO adsorption showed that the addition of potassium decreased the number of adsorption sites, but increased the TOF, indicating the generation of strong active sites. The TOF for the

Table 1
BET surface area for $Ni_{25}Mo_{75}$ catalysts.

Carburization temperature (K)	BET surface area (m^2/g)		CO adsorption (μmol/g)		TOF (min^{-1})	
	$Ni_{25}Mo_{75}$	$Ni_{25}Mo_{75}K_2$	$Ni_{25}Mo_{75}$	$Ni_{24}Mo_{74}K_2$	$Ni_{25}Mo_{75}$	$Ni_{24}Mo_{74}K_2$
798	94 (46)[a]	106 (28)[a]	165	32	1	15
823	146 (53)	47 (34)	70	16	1	31
843	nm (nm)	22 (26)	45	48	8	6
873	47 (31)	4 (2)	30	5	25	57

nm: not measured.
[a] Parentheses: BET surface area of the catalysts after the reaction was measured.

873 K-carburized catalyst was higher than those for the other catalysts, but decreased during the reaction. Concerning the activity of Mo_2C, Solymosi et al. [8,9,21,28] reported that Mo_2C exhibited a lower activity for the cleavage of the C–C bond and higher activity for the rupture of the C-H and O–H bonds with $C_2H_5OH:H_2O = 1:3$ at the reaction temperature of 573–723 K. However, the 873 K-carburized NiMo catalyst favored the C–C bond rupture during the initial stage and the C–O bond rupture that formed ethylene in the final stage due to the oxidation of the NiMo carbides to the oxides under the different conditions of $C_2H_5OH:H_2O = 1:13$ at the reaction temperature of 673 K. Yates and co-workers [23] studied the decomposition of ethanol on Ni(1 1 1) and reported the reactivity order of O–H > C–H (methylene) > C–C > C–H (methyl). Furthermore, the C–O bond on Ni(1 0 0) was not broken [24]. Based on these reports, the C–O bond of ethanol was not broken on the Ni atom, but occurred on the Mo atom of the Mo oxide then scission of the C–C bond of the acetaldehyde. In this study, the reaction steps for the carburized $Ni_{25}Mo_{75}$ catalyst were as follows: (1) Ethanol was adsorbed on the surface. (2) The ethanol was converted to ethoxide species and its C–C bond was ruptured to form acetaldehyde. (3) The C–O bond of the adsorbed ethanol ruptured on the Mo atom, then ethylene was produced.

3.3. XRD analysis for the 823 K-carburized $Ni_{25}Mo_{75}$ and $Ni_{24}Mo_{74}K_2$ before and after the reaction

The XRD patterns of the carburized $Ni_{25}Mo_{75}$ catalysts before and after the reaction are shown in Fig. 7A and B, respectively. The 798 K-carburized $Ni_{25}Mo_{75}$ catalysts consisted of MoO_2 with a small peak of Ni metal, but not NiO. The β-Mo_2C peaks appeared at the carburization temperature of 823 K and became significantly high in intensity at 848 and 873 K. For the all catalysts, the peak at 44.0° was observed due to the formation of Ni metal ($2\theta = 44.5°$, 51.8°, 76.4°, PDF no. 4-0850) or MoNi ($2\theta = 40.8°$, 43.2°, 43.9°, PDF no. 48-1745) which would be formed during incorporation of the Mo atoms into the Ni lattice. As shown by Oku et al. [29], the formation of the NiMo bimetallic alloy decreased the Ni 2p satellite peak, and alloying of the NiMo donors electrons to the 3d orbital to decrease the satellite peak due to the donation of electrons from Ni to Mo. Based on the results, the peak at 44.0° was attributed to the Ni metal and NiMo. The β-Mo_2C in the fresh carburized 798 and 823 K-carburized catalysts turned to MoO_2, but for the 873 and 848 K-carburized catalysts, the β-Mo_2C was not changed. Concerning the potassium-added catalysts (Fig. 7C and D), the 798 K-carburized catalyst exhibited high intensity peaks of MoO_2, and small peaks of β-Mo_2C and Ni metal (or NiMo) were present, while

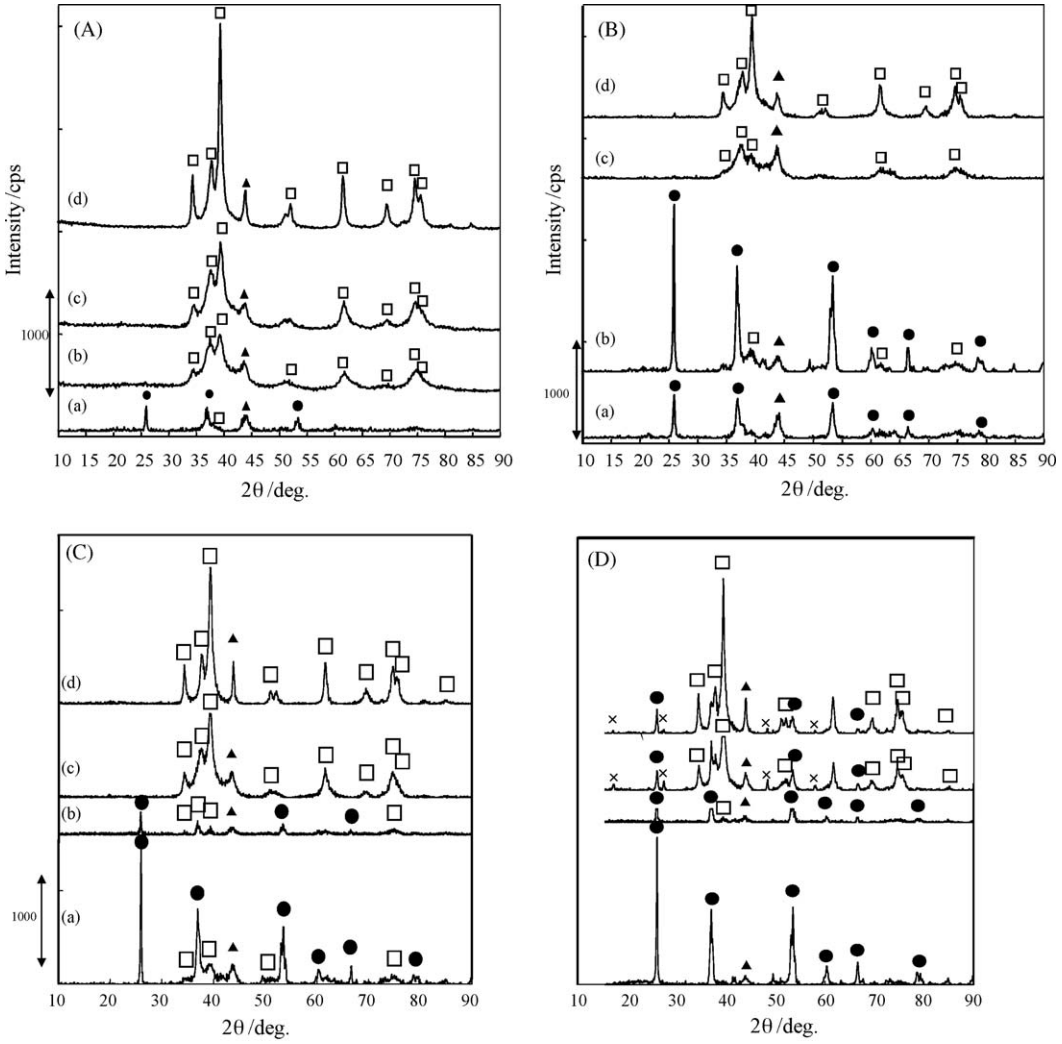

Fig. 7. (A and B) XRD patterns of $Ni_{25}Mo_{75}$ carburized (a) 798, (b) 823, (c) 848 and (d) 873 K (A) before and (B) after the reaction. (●) MoO_2, (□) β-Mo_2C and (▲) Ni metal (MoNi). (C and D) XRD patterns of $Ni_{24}Mo_{74}K_2$ carburized (a) 798, (b) 823, (c) 848 and (d) 873 K (C) before and (D) after the reaction. (●) MoO_2, (□) β-Mo_2C, (▲) Ni metal (MoNi) and (×) $K_2Mo_8O_{16}$.

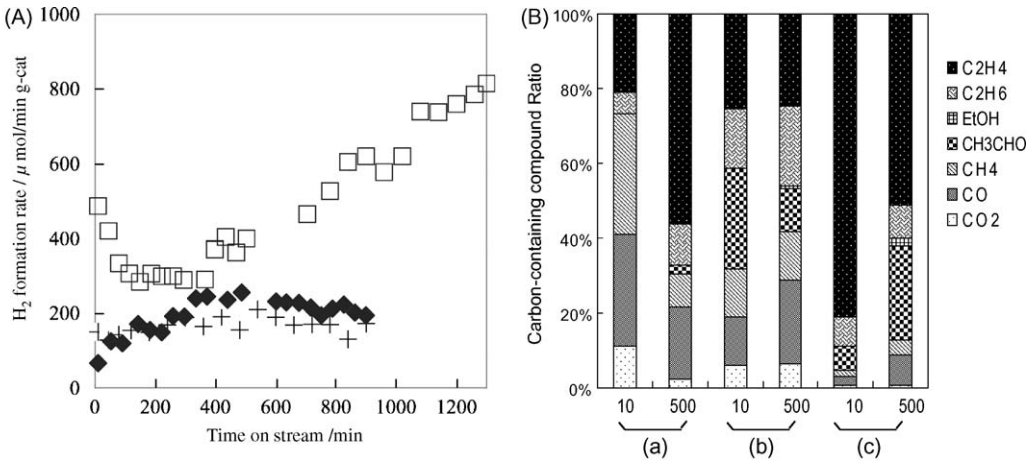

Fig. 8. (A) Formation rate of hydrogen over the (◆) 823 K-carburized $Ni_{25}Mo_{75}$ catalyst, (□) 823 K-carburized $Ni_{24}Mo_{74}K_2$ and (+) 823 K-reduced $Ni_{25}Mo_{75}$ and (B) product distribution over the (a) 823 K-carburized $Ni_{25}Mo_{75}$ catalyst, (b) 823 K-carburized $Ni_{24}Mo_{74}K_2$ and (c) 823 K-reduced $Ni_{25}Mo_{75}$ catalyst at reaction temperature of 673 K.

the 823 K-carburized catalyst showed broad and small peaks. The 873 and 848 K-carburized catalysts contained a strong intensity of β-Mo_2C and Ni metal (or NiMo). After the reaction, the $Ni_{24}Mo_{74}K_2$ catalysts contained Mo oxides and $K_2Mo_8O_{16}$, which were formed by reaction of potassium with MoO_2 during the reaction for even the catalysts carburized at 848 and 873 K, but not at low temperatures of 798 and 723 K. Consequently, the 823 K-carburized $Ni_{24}Mo_{74}K_2$ catalyst with a high activity for hydrogen formation during the initial step contained large crystals of MoO_2 with β-Mo_2C and Ni^0 metal (or NiMo) as well as the 798 K-carburized $Ni_{25}Mo_{75}$ catalyst.

3.4. Comparison of carburized catalyst with reduced catalyst

The 823 K-carburized $Ni_{25}Mo_{75}$ catalysts with and without potassium compared to the 823 K-reduced $Ni_{25}Mo_{75}$ catalyst in the ethanol steam reforming at 673 K is shown in Fig. 8. The hydrogen formation of these catalysts was very similar, although almost constant for the carburized catalyst during the reaction. For the reduced catalyst (Fig. 8B), the formation rate was initially low, the ethylene selectivity was 0.8 at 10 min, but the acetaldehyde selectivity increased at 500 min. The carburized catalyst exhibited a high selectivity for ethylene during the reaction. The carburized catalyst had more CO and CH_4 formation than the reduced catalyst with hydrogen due to enhancing the reforming of acetaldehyde (C–C bond scission).

The interactions of ethanol with the surface of the 823 K-carburized $Ni_{25}Mo_{75}$ and $Ni_{24}Mo_{74}K_2$ and the 823 K-reduced $Ni_{25}Mo_{75}$ catalysts were investigated by the TPSR experiment of ethanol as shown in Fig. 9. All the peaks of the products for the 823 K-reduced $Ni_{25}Mo_{75}$ were observed at a lower intensity than those for the two carburided catalysts. The hydrogen peaks appeared at 490 and 700 K for the 823 K-carburized $Ni_{25}Mo_{75}$ catalyst, and they were extremely increased for the $Ni_{24}Mo_{74}K_2$ catalyst. Hydrogen was formed along with CO_2 and CH_4 in the range of 550–830 K for both carburized catalysts. Considering the latter large hydrogen peaks, these desorptions would indicate the decomposition of acetaldehyde and the water gas shift reaction conversion of methane to hydrogen and CO_2 for $Ni_{24}Mo_{74}K_2$. It shows that the potassium addition promoted the C–C bond cleavage based on the TPSR analysis. For the $Ni_{25}Mo_{75}$ reduced at 823 K, the low intensity hydrogen peaks of 590 and 740 K were observed at lower values than the peaks for the two carburided catalysts. The ethylene, ethane and acetaldehyde peaks at 580 K were observed to be greater than the corresponding peaks for the 823 K-carburized $Ni_{25}Mo_{75}$, but no CO and CO_2 were observed. Thus, the 823 K-reduced $Ni_{25}Mo_{75}$ possessed little capacity for the C–C bond cleavage at low temperature. Based on the TPSR analysis, the carburized $Ni_{24}Mo_{74}K_2$ catalyst produced more hydrogen than the reduced catalyst at low temperature.

3.5. Composition by XPS and active sites

The XRD measurements revealed that the catalyst carburized at 798 K with the highest activity was formed from MoO_2, β-Mo_2C and Ni^0 metal (or NiMo). The 873 K-carburized Ni_{100} and Ni_2Mo_{98} catalysts were extremely promoted for the hydrogen formation compared to the Mo_{100} catalyst containing MoO_2 which exhibited little activity at 773 K. Thus, this suggests that the nickel or NiMo on the surface was active for the hydrogen formation during the reaction, but the active species for the ethanol steam reforming have not been fully understood based on the compositions of the bulk by XRD. The surface compositions of the $Ni_{25}Mo_{75}$ and $Ni_{24}Mo_{74}K_2$ carburized at the various temperatures and analyzed by the XPS experiments are shown in Figs. 10 and 11. The XPS binding energies of the XPS Mo $3d_{5/2}$ and $3d_{3/2}$ lines and Ni $3d_{5/2}$ and $3d_{3/2}$ lines before the reaction are shown in Fig. 10. The Mo^{2+} and Mo^{3+} ions of the $Ni_{25}Mo_{75}$ were distributed at more than 60% due to the β-Mo_2C identified from the XRD analysis. Although this distribution increased with the increased carburization temperature, for the 798 K-carburized catalyst, Mo^0 and Mo^{2+} were observed. MoO_2 was mainly detected by the XRD measurement, that is, suggesting large content of Mo^{4+}. Furthermore, for the Ni composition, Ni^{3+} and Ni^{2+} were mostly distributed and increased at the higher carburization temperatures. As the Ni probably donates electrons to Mo for the nickel molybdenum compounds [21], the nitrogen donates electrons to Mo and then distribution of the Ni^{3+}, Mo^0 and Mo^{2+} increased. On the other hand, for the potassium-added catalysts (Fig. 11), the distributions of the Mo^{5+} and Mo^{6+} increased when compared to the non-potassium-added catalysts. The Mo^{2+} ion decreased for the 798 and 823 K-carburized catalysts, while the Mo^{3+} and Mo^{4+} ions significantly decreased for the 848 and 873 K-carburized catalysts, suggesting the formation of oxycarbides (MoO_xC_y and/or $NiMoO_xC_y$) or a compound that reacted with potassium. Juan-Juan et al. [30] reported that the potassium addition increased the distribution of Ni^0 and the reducibility of nickel. This increase in the Ni valence and the decrease in the Mo valence were attributed to the increase in the electron donation of potassium to nickel and the Ni reducibility. Furthermore, the Ni^{2+} satellite peak intensity of the 823–873 K-carburized catalysts with potassium decreased. The formation of the NiMo bimetallic alloy decreases the Ni 2p satellite peak,

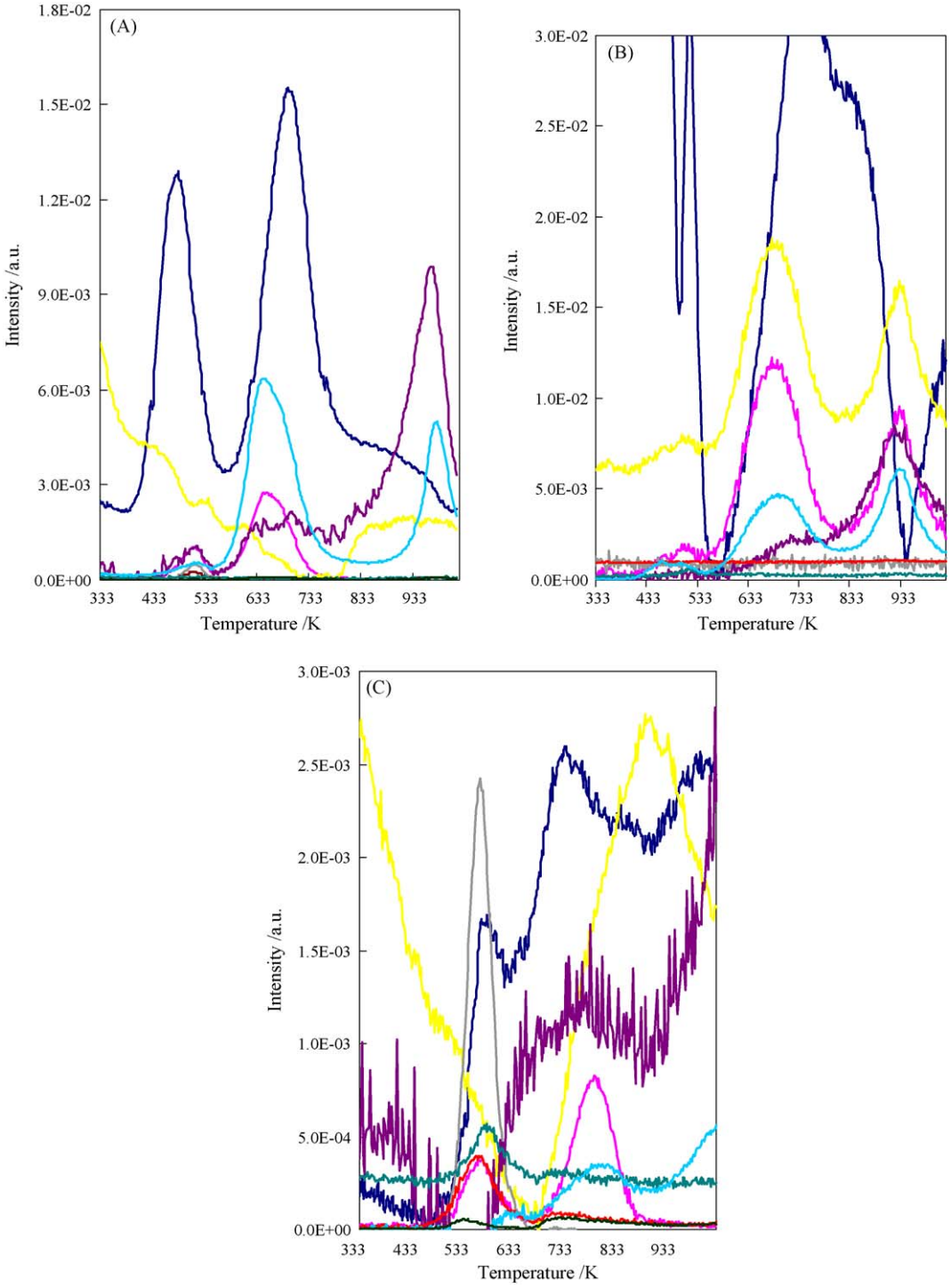

Fig. 9. TPSR spectra for (A) 823 K-carburized $Ni_{25}Mo_{75}$, (B) 823 K-carburized $Ni_{24}Mo_{74}K_2$ and (C) 823 K-reduced $Ni_{25}Mo_{75}$ and after the ethanol adsorption. (▬) H_2, (▬) CH_4, (▬) H_2O, (▬) C_2H_4, (▬) CO, (▬) CH_3CHO, (▬) C_2H_6, (▬) CO_2 and (▬) ethanol.

alloying of NiMo donor electrons to the 3d orbital to decrease the satellite peak due to the reaction of Ni with potassium, the electron donor of potassium to nickel and the donation of electrons from Ni to Mo [29]. Furthermore, Sehested et al. [31] found that the presence of potassium decreased the surface free energy of Ni and accelerated the transfer of Ni to other species, resulting in the sintering of Ni. In this study, the carburized catalysts had a low surface area because of Ni sintering in agreement with the sharper peaks of the Ni species Bengaard et al. [32] studied the DFT calculation of potassium behavior of the Ni catalyst and reported that the potassium preferentially and highly reacted with "step sites" rather than "terrace sites", resulting in the prevention of the dissociation of the C–H bond of CH_4 and carbon deposition. This behavior resulted in promotion of the activity for the hydrogen production during the ethanol steam reforming. Moreover, the 848 and 873 K-carburized catalysts exhibited a high activity during the initial stage of the reaction, but the potassium addition did not show any high activity but a stable production of hydrogen. The XRD and XPS analyses showed that the potassium addition prevented the formation of the Mo carbide. Furthermore, the

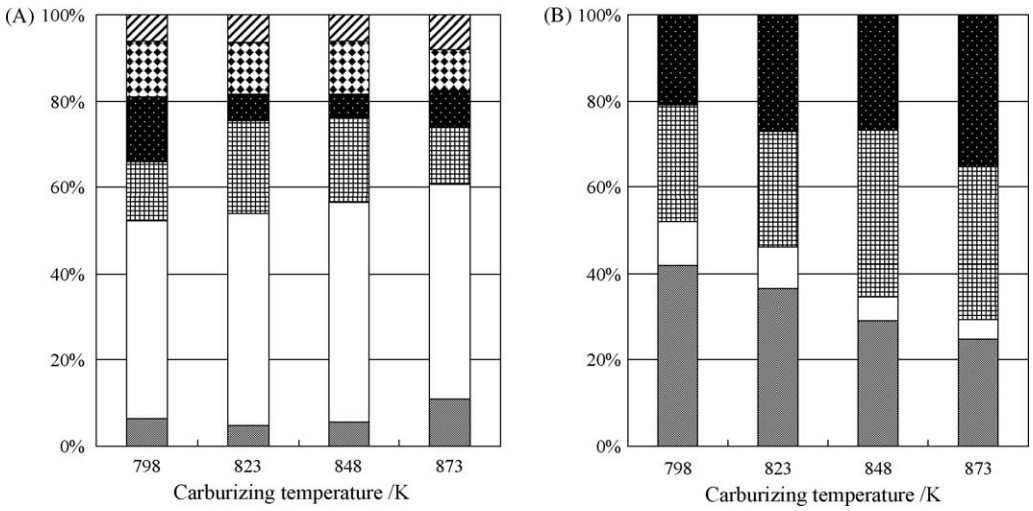

Fig. 10. Distribution of (A) Mo^{x+} and (B) Ni^{y+} ions for $Ni_{25}Mo_{75}$ carburized at 798, 823, 848, and 873 K before the reaction. (▨) Mo^{6+}, (▦) Mo^{5+}, (▨) Mo^{4+}, (■) Mo^{3+}, (□) Mo^{2+} and (▩) Mo^0. (▩) Ni^{2+} sat, (▦) Ni^{3+}, (□) Ni^{2+} and (■) Ni^0.

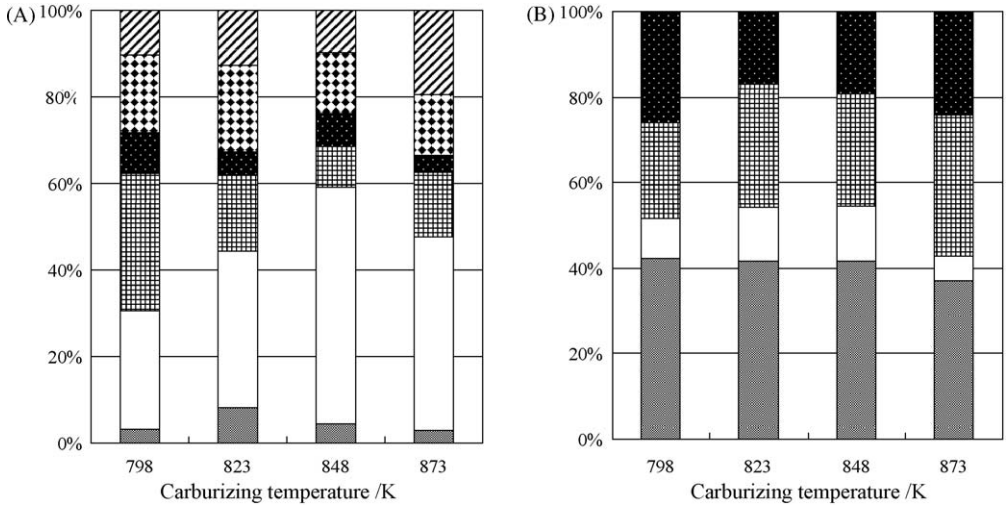

Fig. 11. Distribution of (A) Mo^{x+} and (B) Ni^{y+} ions for $Ni_{24}Mo_{74}K_2$ carburized at 798, 823, 848, and 873 K before the reaction. (▨) Mo^{6+}, (▦) Mo^{5+}, (▨) Mo^{4+}, (■) Mo^{3+}, (□) Mo^{2+} and (▩) Mo^0. (▩) Ni^{2+} satellite, (▦) Ni^{3+}, (□) Ni^{2+} and (■) Ni^0.

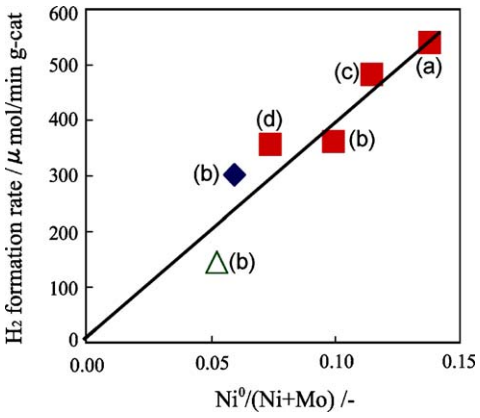

Fig. 12. Relationship between H_2 formation rate and $Ni^0/(Ni + Mo)$ ratio of the (◆) 823 K-carburized $Ni_{25}Mo_{75}$, (■) 798–873 K-carburized $Ni_{24}Mo_{74}K_2$ and (△) 823 K-reduced $Ni_{25}Mo_{75}$. Carburization temperatures: (a) 798, (b) 823, (c) 848 and (d) 873 K.

TOF during the initial stage was the highest value for the 873 K-carburized $Ni_{24}Mo_{74}K_2$ which contained β-Mo_2C, Ni metal (or NiMo) and Mo (NiMo) oxycarbides. Based on these results, the strong active sites of the 873 K-carburized $Ni_{24}Mo_{74}K_2$ would be proposed as N^0 of Ni metal (or NiMo) that interacted with β-Mo_2C. β-Mo_2C was converted to Mo oxide during the reaction. The carburized $Ni_{25}Mo_{75}$ and $Ni_{24}Mo_{74}K_2$ exhibited similar TOFs, suggesting the presence of Ni metal that interacted with Mo (oxy)carbide and MoO_2. Therefore, highly dispersed small particles of Ni^0 metal with NiMo on Mo_2C were contained in the $Ni_{24}Mo_{74}K_2$ catalyst, and then Ni^0 was stable due to the preferential oxidation of the Mo of β-Mo_2C and Mo oxycarbide during the reaction. The relationship between the ratio of the hydrogen formation rate and the nickel (Ni^0) ratio is shown in Fig. 12. The equilateral correlation between the Ni/(Ni + Mo) ratio and the produced hydrogen amount was observed. Thus, the Ni^0 of the Ni metal and/or NiMo was the active species for the ethanol steam reforming. The Ni content was not increased for the $Ni_{25}Mo_{75}$ catalysts, but for the $Ni_{24}Mo_{74}K_2$ catalysts, it increased during the reaction for the Ni^0/(Ni + Mo) ratio of 0.07–0.14 for the 798 K-carburized $Ni_{24}Mo_{74}K_2$

catalyst, although the 873 K-carburized $Ni_{24}Mo_{74}K_2$ catalyst had the Ni^0/(Ni + Mo) ratio of 0.13–0.07. This result showed that the nickel atoms were covered with many carbons before the reaction, but the carbons were removed during the reaction and the exposed Ni atomic ratio increased. Consequently, the $Ni_{24}Mo_{74}K_2$ catalysts contained highly dispersed small particles of Ni^0 metal (and/or NiMo) on the Mo oxycarbide and the β-Mo_2C and Ni^0 were stable (migration of Ni from balk to the surface for the 798 K-carburized catalyst) due to the preferential oxidation of the low valence to the high valence of the Mo atoms of the Mo oxides during the reaction.

4. Conclusion

The NiMo carburized catalysts and the promoting effect of potassium were studied for the ethanol steam reforming at 673 K and then compared to the reduced catalyst. The effects of the nickel content, reaction temperature and carburization temperature on the product selectivity during the ethanol steam reforming was also determined. The active sites were characterized by TPSR, XRD and XPS measurements. The 798 K-carburized catalyst undergoes C–O bond cleaved rather than the catalysts carburized at high temperature. For the 873 K-carburized catalyst, the C–C bond of the converted acetaldehyde was cleavaged only during the initial stage, but was suppressed with the increased activity for the C–O bond cleavage during the reaction. As a result, the C–O bond cleavage was related to an oxide and the C–C bond cleavage was related to a carbide. The potassium-added $Ni_{24}Mo_{74}K_2$ carburized at 798 K was the most active for the hydrogen production. The addition of potassium to the catalyst was effective for the O–H bond scission (acetaldehyde selectivity) with less C–O bond scission (ethylene selectivity) and a long and stable steam reforming reaction. The steam reforming of ethanol proceeds with the dehydrogenation to acetaldehyde (O–H scission) or the dehydration to ethylene (C–O bond scission). The C–C bond scission of acetaldehyde occurred and then formed CH_4 and CO (C–C bond scission). The water gas CO shift reaction and steam reaction of methane occurred. The addition of potassium resulted in the increase in the electron donation of potassium to nickel and Ni reduction and the reaction of Ni with potassium as well as the donation of electrons from Ni to Mo for the carburization of the NiMo compounds. The $Ni_{24}Mo_{74}K_2$ catalysts contained highly dispersed small particles of Ni^0 metal (and/or NiMo) on the Mo oxycarbide, and the β-Mo_2C and Ni^0 were stable due to the preferential oxidation of the low valence to the high valence of the Mo atoms of the Mo oxides during the reaction. This carburization treatment of the NiMo catalysts offers the possible preparation of a good catalyst for hydrogen production from bioethanol.

References

[1] National Geographic, 36, October 2007.
[2] F. Aupreetre, C. Descorme, D. Duprez, Catal. Commun. 3 (2002) 263.
[3] J. Sun, X.-P. Qiu, F. Wu, W.-T. Zhu, Int. J. Hydrogen Energy 30 (2005) 437.
[4] F. Frusteri, S. Freni, V. Chiodo, L. Spadaro, O. Di Blasi, G. Bonura, S. Cavallaro, Appl. Catal. A 270 (2004) 1.
[5] A.J. Vizcaino, A. Carrero, J.A. Calles, Int. J. Hydrogen Energy 32 (2007) 1450.
[6] F. Arena, F. Frusteri, A. Parmaliana, Appl. Catal. A: Gen. 187 (1999) 127.
[7] A.N. Fatsikostas, X.E. Verykios, J. Catal. 225 (2004) 439.
[8] R. Barthos, A. Széchenyi, F. Solymosi, Catal. Lett. 120 (2008) 161.
[9] J. Sun, X. Qiu, F. Wu, W. Zhu, W. Wang, S. Hao, Int. J. Hydrogen Energy 29 (2004) 1075.
[10] D. Srinivas, C.V.V. Satyanarayana, H.S. Potdar, P. Patnasamy, Appl. Catal. A: Gen. 246 (2003) 323.
[11] J. Llorca, N. Homs, J. Sales, P.R. de la Piscina, J. Catal. 209 (2002) 306.
[12] F. Aupretre, C. Descorme, D. Duprez, D. Casanave, D. Uzio, J. Catal. 233 (2005) 464.
[13] J.P. Breen, R. Burch, H.M. Coleman, Appl. Catal. B: Environ. 39 (2002) 65.
[14] M. Patterson, T.K. Das, B.H. Davis, Appl. Catal. A: Gen. 251 (2003) 449.
[15] J. Patt, D.J. Moon, C. Phillips, L. Thompson, Catal. Lett. 65 (2000) 193.
[16] M. Nagai, T. Nishibayashi, S. Omi, Appl. Catal. A: Gen. 253 (2003) 101.
[17] K. Oshikawa, M. Nagai, S. Omi, J. Phys. Chem. B 105 (2003) 9124.
[18] M. Nagai, K. Matsuda, J. Catal. 238 (2006) 489.
[19] D.J. Moon, J.W. Ryu, Catal. Lett. 92 (2004) 17.
[20] R. Barthos, A. Szechenyi, A. Koos, F. Solymosi, Appl. Catal. A: Gen. 327 (2007) 95.
[21] A.P. Farkas, F. Solymosi, Surf. Sci. 602 (2008) 1475.
[22] M. Nagai, A.M. Zahidul, K. Matsuda, Appl. Catal. A: Gen. 313 (2006) 137.
[23] S.M. Gates, J.N. Russel Jr., J.T. Yates Jr., Surf. Sci. 171 (1986) 111.
[24] Th. Kratochwil, M. Wittmann, J. Küppers, J. Electron Spectrosc. Relat. Phenom. 64/65 (1993) 609.
[25] T. Osaki, T. Mori, J. Catal. 204 (2001) 89.
[26] H. Tominaga, M. Nagai, J. Phys. Chem. B 109 (2005) 20415.
[27] Q. Zhu, B. Zhang, J. Zhao, S. Ji, J. Yang, J. Wang, H. Wang, J. Mol. Catal. A: Chem. 213 (2004) 199.
[28] A. Széchenyi, F. Solymosi, J. Phys. Chem. C 111 (2007) 9509.
[29] M. Oku, H. Tokuda, K. Hirokawa, J. Electron Spectrosc. Relat. Phenom. 53 (1991) 201.
[30] J. Juan-Juan, M.C. Román-Mantinez, M.J. Illán-Gómez, Appl. Catal. A: Gen. 264 (2004) 169.
[31] J. Sehested, J.A.P. Gelten, S. Helveg, Appl. Catal. A: Gen. 309 (2006) 237.
[32] H.S. Bengaard, J.K. Nørskov, J. Sehested, B.S. Clausen, L.P. Nielsen, A.M. Molenbroek, J.R. Nielsen, J. Catal. 209 (2002) 365.